Available online at www.sciencedirect.com

ScienceDirect

Mendeleev Commun., 2020, **30**, 805–808

Mendeleev Communications

Effect of albumin on the aggregation of deuteroporphyrin in aqueous organic medium

Natalya Sh. Lebedeva, Elena S. Yurina, Yury A. Gubarev* and Sabir S. Guseinov

G. A. Krestov Institute of Solution Chemistry, Russian Academy of Sciences, 153045 Ivanovo, Russian Federation. E-mail: yury.gu@gmail.com

DOI: 10.1016/j.mencom.2020.11.039

In water–DMF at DMF content less than 2.6 mol dm^{-3}, deuteroporphyrin IX dimethyl ester forms both H- and J-aggregates. The J-aggregates are detected as a single type of associated species after binding of the porphyrin with BSA on the surface of the protein IB subdomain.

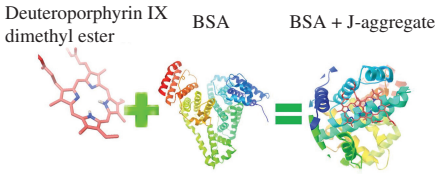

Keywords: deuteroporphyrin, albumin, aggregation, UV-VIS, fluorescence, molecular docking, J-aggregate.

Porphyrins attract much attention due to expanding opportunities for their use in medicine, biomimetic chemistry and material science,[1–4] including solar energy conversion.[5,6] Electronic and spectroscopic properties as well as the related application of porphyrins depend largely on their self-aggregation, therefore great efforts have been made recently to investigate the association of these compounds. Generally, porphyrins can form two types of non-covalent aggregates in aqueous medium, namely H- and J-aggregates.[7] The latter represent typically a dimeric form, higher associates being insoluble in water. In the H-aggregates, porphyrin molecules are in a 'face-to-face' arrangement and their aromatic systems overlap completely, whereas in the J-aggregates the molecules are located next to each other 'side-by-side' (or 'edge-to-edge') and the aromatic moieties do not interact. As follows from quantum-chemical calculations,[8] the distance between porphyrin macrocyclic planes in H-dimers is 3.2–3.8 Å, which indicates a π–π-interaction. On the contrary, the interplanar distance in J-dimers is more than 5 Å, which excludes the π–π-interplay. UV-VIS spectral patterns of the H- and J-aggregated species vary significantly, the H-aggregation causes a blue shift of absorption bands, while the formation of J-dimers is accompanied by a red shift of the corresponding bands up to 50 nm. The absence of π–π-interaction in J-dimers allows an investigation of their own fluorescence.

Understanding the mechanism of J-aggregation and its dependence on conditions determining the location and orientation of chromophores represents a promising issue for tuning optical and electronic properties as well as for design of new optical materials. According to the known works, porphyrins protonation contributes to the formation of extended J-aggregates, so these associates of water-soluble porphyrins are formed mainly in acidic medium.[9–12] The distorted planar structure of diprotonated porphyrin prevents a coplanar π–π-interaction between their aromatic systems and thus does not allow the formation of H-aggregates. Only a few publications report the formation of J-aggregates at neutral pH.[13–15] One of them emphasizes a cationic porphyrins origin of the J-aggregates at pH = 7,[13] where the association occurs in the presence of iodide ion under light irradiation and a mechanism includes singlet oxygen generation by porphyrin followed by oxidation of iodide ion to I^{3-} by singlet oxygen with further formation of porphyrin–I^{3-} ion pairs in solution. A lot of data is available for polycations as initiators of the formation of J-aggregates from water-soluble porphyrins.[16,17] Thus, for water-soluble and amphiphilic porphyrins, an interaction with counter ions, other electrolytes and polyelectrolytes affects the self-aggregation.[18]

Concerning hydrophobic porphyrins, their J-aggregation was reported, for example, as the interaction of protoporphyrin IX with human serum albumin and transferrin with formation of J-aggregates in a concentration range of porphyrin $1–2\times10^{-3}$ mmol dm^{-3}.[19] The complex multicomponent systems consisting of two proteins, Lomefloxacin drug and protoporphyrin in borate buffer were studied there, and the J-aggregation was not explored in detail.

The aim of this work was to investigate the formation of J-dimers from dimethyl 3,7,12,17-tetramethyl-21*H*,23*H*-porphine-2,18-dipropionate (deuteroporphyrin IX dimethyl ester, H_2DP) upon binding to bovine serum albumin (BSA).[†]

Due to hydrophobicity of H_2DP, DMF was used as a cosolvent. The DMF content in the solution with BSA did not exceed 0.19 mol dm^{-3}, which could not affect a native conformation and

[†] BSA fraction V (Acros Organics), H_2DP (Sigma–Aldrich), double distilled water and freshly distilled DMF (Chimmed, Russia) were employed. NaCl (Reakhim, Russia, >99%) was additionally recrystallized.

UV-VIS absorption and fluorescence spectra were recorded using an AvaSpec-2048 double channel spectrophotometer (Avantes BV, Netherlands) at 25 °C in 1 cm quartz cuvettes. An UVTOP295 (Sensor Electronic Technology, Inc., USA) and a VL425-5-15 (Roithner LaserTechnik GmbH, Germany) monochromatic LEDs were employed as fluorescence excitation light sources.

Particle size was measured by DLS using a Zetasizer Nano instrument (Malvern Panalytical, UK).

TG and DTG investigations were carried out on a TG 209 F1 thermomicrobalance (Netzsch-Gerätebau GmbH, Germany) as follows. H_2DP DMF solvate (9.55 mg, initial ratio 1 : 27) was placed into a platinum crucible and heated from room temperature to 250 °C at 10 °C min^{-1} rate in a dry Ar flow of 30 ml min^{-1}.

DSC study was performed using a DSC 204 F1 instrument (NETZSCH-Gerätebau GmbH, Germany). Test sample (5.75 mg) was placed in a pressed aluminum crucible with a hole in the cover. Two empty aluminum crucibles were used as references. The calorimetric experiment was carried out at heating rate of 10 °C min^{-1} in a dry Ar flow of 40 ml min^{-1}. All the DSC measurements were performed relative to a baseline obtained for the references.

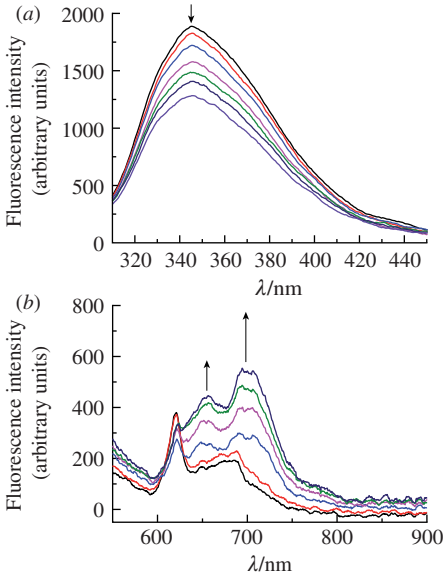

Figure 1 Corrected fluorescence spectra upon titration of 0.08 wt% BSA solution with 0 to 4×10^{-6} M H_2DP at (*a*) λ_{ex} = 296 nm and (*b*) λ_{ex} = 425 nm.

properties of the protein.[20] H_2DP was dissolved in DMF and then an aliquot of the solution with a known concentration of DMF was introduced into the protein solution (0.08 wt% BSA and 0.05 mol dm^{-3} NaCl in water). Thus, we used the known strategy of porphyrin aggregation initiation, where the porphyrin was first dissolved in a 'good' solvent and then in a 'bad' solvent. Note that in the absence of BSA we failed to obtain any resistant to sedimentation solutions of H_2DP in water containing 0.05 mol dm^{-3} NaCl and 0.19 mol dm^{-3} DMF. In contrast, in the presence of BSA the porphyrin solutions were stable for 1–2 weeks in a refrigerator. Figure 1(*a*) demonstrates typical changes in BSA fluorescence upon porphyrin titration, with the protein fluorescence at λ_{ex} = 295 nm originating from Trp(134) and Trp(214) residues of the albumin polypeptide chain. An increase in the concentration of BSA is accompanied by quenching of its fluorescence, which indicates the interaction between the protein and the porphyrin [see Figure 1(*a*)]. For an effective fluorescence quenching, the distance between a quencher and a fluorophore should not exceed 20 Å. Here, the quenching is not complete and the porphyrin quencher is likely bound to the BSA site containing only one of the two Trp residues. The Trp(134) residue is known to be located in the subdomain IB, where a heme site of BSA is also included, while the Trp(214) residue is located in subdomain IIA (*i.e.*, binding site I according to Sudlow[22]).

The change in fluorescence spectra of H_2DP for the same experimental series at another λ_{ex} = 425 nm is shown in Figure 1(*b*). An increase in the porphyrin concentration leads to significant variation of the fluorescence spectrum already at 1.6×10^{-6} mol dm^{-3} H_2DP, with inversion of band intensities along with a shift of the fluorescence maxima to the far spectral region. UV-VIS absorption spectrum of porphyrin also changes on going from DMF to an aqueous organic medium (Figure 2). The absorption intensity decreases and broadening occurs in the region of a Soret band (the intensive absorption at less than 300 nm originates from BSA). The bands resolution in the far spectral part decreases and the spectrum transforms into a two-bands one. These spectral changes along with the presence of fluorescence from aggregated forms of porphyrin represent a hallmark of J-aggregation. A

‡ For diluted solutions of H_2DP, fluorescence intensity was not corrected because the optical density did not exceed 0.1. For concentrated solutions, the fluorescence intensity was corrected for inner filter and dilution effects before the data analysis.[21]

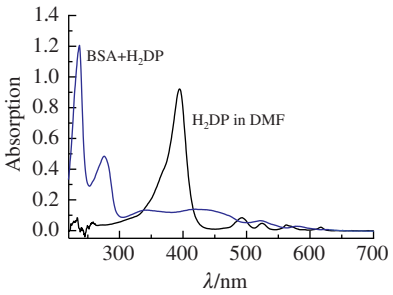

Figure 2 UV-VIS absorption spectrum of H_2DP in DMF as well as H_2DP–BSA mixture in aqueous solution containing 0.05 M NaCl and 0.19 M DMF.

question arises, whether the formation of J-aggregates originates from the medium or from the interaction with BSA.

To clarify this, we carried out additional spectral as well as thermogravimetric investigations of the H_2DP solvation in an aqueous–organic medium with various DMF content. The changes in the H_2DP UV-VIS absorption and fluorescence spectra with the DMF amount decrease are collected in Table S1 (see Online Supplementary Materials). The obtained spectral data revealed that H_2DP aggregates at low DMF content and at more than 4.31 mol dm^{-3} DMF π–π-aggregates of the porphyrin were formed. With a decrease in the concentration of DMF to 2.58 mol dm^{-3}, J-aggregates appeared along with the π–π-aggregates. Further lowering of the DMF content to 0.69 mol dm^{-3} led to a reduction in the amount of π–π-aggregates as well as an increase in the content of J-dimers. Note that the H_2DP solubility simultaneously decreased and with a further lowering of DMF amount, the solution became unstable to sedimentation at storage. According to DLS data, large porphyrin aggregates with a hydrodynamic diameter of ~1350 nm were mainly present in the solution containing 0.4 mol dm^{-3} DMF.

The transition from four- to two-band absorption pattern in the far visible spectral part indicates a transfer to higher symmetry of the porphyrin molecule, namely from D_{2h} to D_{4h} one.[23] This is possible due to the donor–acceptor interactions of hydrogen atoms of pyrrole moieties with electron donor ligands or, alternatively, to protonation of nitrogen atoms in the macro ring.[24]

According to the thermogravimetric analysis data, desolvation/dehydration of the H_2DP crystal solvates from DMF and DMF–H_2O proceed stepwise (Figure 3). For both solvents at the first step up to 120 °C their molecules with a universal character of interaction with porphyrin[25] are removed. At the second step in the temperature range of 140–164 °C [Figure 3(*a*)], the DMF molecules, which specifically solvate the porphyrin, are removed and the composition of H_2DP–DMF solvate is calculated to be 1 : 2 [see Figure 3(*a*)]. As follows from this ratio, the DMF molecule interacts with the porphyrin at its reaction center. Therefore, coordinated or oriented DMF molecules can hinder the coplanar π–π-interaction and contribute to the formation of J-aggregates. It was impossible to deduce the composition of the corresponding solvate for the aqueous organic solvent, however taking into account the hydrophobic nature of H_2DP and a similar desolvation pattern at the second step with the temperature of maximum mass loss rate of 149.6 °C [see Figure 3(*a*), DTG curve] as well as the endothermic peak in DSC curve at 143.8 °C [Figure 4(*b*)], it could be assumed that for the mixed solvent at the second step the DMF molecules, which had been specifically bound to porphyrin, were removed.

Known data concerning the initiation of porphyrin aggregation by proteins or amino acids raises more questions than provides answers. For amino acids, the issue is less ambiguous, namely depending on the amino acid isoelectric point and pH, a carboxyl or amino group is protonated, so water-soluble porphyrins become

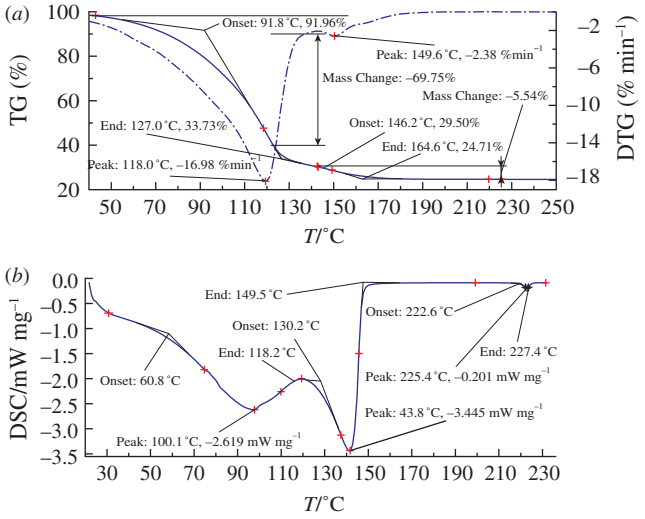

Figure 3 (*a*) TG and DTG curves for the H_2DP–DMF solvate as well as (*b*) DSC curve for the H_2DP–DMF–H_2O solvate.

oriented relative to the amino acid molecule by electrostatic interactions, and thus the chiral J-aggregates are formed.[26] The same principle is applied to cationic or anionic polymers, which form micelles 'sheathed' by the porphyrin J-aggregates.[27,28] Employment of this pattern for proteins with their complicated non-repeating structure has some advantages, because a protein can have a negative or positive surface charge depending on pH of the medium and the isoelectric point. So, BSA with p*I* = 4.6 at pH < 4.6 acquires a positive charge and attracts for example anionic sulfoporphyrins.[29] Coulomb interactions lead to partial neutralization of converging porphyrin anions, facilitating the formation of J-aggregates.[29] Nevertheless, in this work similar to articles[21,30] the BSA-initiated formation of J-dimers of porphyrins is proved, and here the electrostatic interactions cannot represent the driving force for aggregation, since porphyrins are in molecular, *i.e.*, uncharged, form. In our opinion, the reason for the BSA-initiated J-dimerization consists in the formation of H-bonds between the porphyrin peripheral substituents, namely $–(CH_2)_2COOMe$, and the BSA amino acid residues, which leads to an increase in the local concentration of the porphyrin in a single region of the protein, *i.e.*, either binding site or a site on the surface of the BSA globule. This interaction along with hydrophobic forces contributes to the porphyrin aggregation.

Molecular docking[§] confirms the main provisions above on the localization of the porphyrin J-dimer next to only one of the Trp residues, the presence of a specific interaction between the H_2DP peripheral substituents and BSA as well as allows visualization of the complex formed (Figure 4). For the J-dimer, the affinity of H_2DP for BSA is 11.6 kcal mol^{-1}, while for the π–π-dimer it is only 7.2 kcal mol^{-1}.

In summary, H_2DP forms both π–π- and J-aggregates in a water–DMF mixed solvent. The J-aggregates are detected at concentration of DMF in the mixed solvent less than 2.6 mol dm^{-3}. However, under these conditions they are present as a mixture with their π–π conterparts. As a single type of aggregated species, the J-dimers are formed *via* binding of 4×10^{-7} to 4×10^{-6} mol dm^{-3} H_2DP with BSA on the surface of its subdomain IB near the Trp(134) residue. The results obtained help in understanding the

§ Molecular Docking was carried out using an AutoDock Vina program.[31] For the calculations, we used structures of J- and π–π-dimers of H_2DP minimized by the semi-empirical method with a Gaussian 09 Revision A.02 software.[32] For visualization, a Python Molecular Viewer version 1.5.6 was employed.

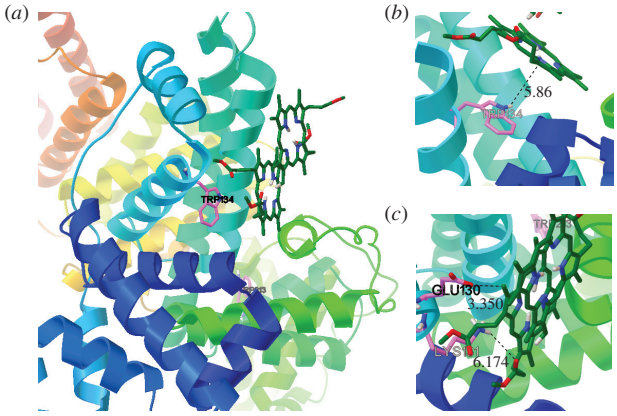

Figure 4 H_2DP J-dimer complex with BSA: (*a*) localization of the J-dimer in the BSA subdomain IB. (*b*),(*c*) Detailed views of the binding mode, the distance between the porphyrin macro ring plane and the Trp(134) residue as well as orientation of the peripheral H_2DP substituents with respect to the BSA amino acid residues.

albumin–porphyrin interaction in blood as well as the aggregated porphyrin properties promising for material science applications.

This work was supported by the Russian Foundation for Basic Research (grant no. 19-03-00468). We are grateful to 'The Upper Volga Region Centre of Physico-Chemical Research' for analysis of the samples investigated.

Online Supplementary Materials

Supplementary data associated with this article can be found in the online version at doi: 10.1016/j.mencom.2020.11.039.

References

1 M. Imran, M. Ramzan, A. K. Qureshi, M. A. Khan and M. Tariq, *Biosensors*, 2018, **8**, 95.
2 K. B. Guterres, G. G. Rossi, L. B. Menezes, M. M. A. de Campos and B. A. Iglesias, *Tuberculosis*, 2019, **117**, 45.
3 J. S. Lindsey, S. Prathapan, T. E. Johnson and R. W. Wagner, *Tetrahedron*, 1994, **50**, 8941.
4 N. T. Anderson, P. H. Dinolfo and X. Wang, *J. Mater. Chem. C*, 2018, **6**, 2452.
5 Ö. Birel, S. Nadeem and H. Duman, *J. Fluoresc.*, 2017, **27**, 1075.
6 J. Lu, H. Li, S. Liu, Y.-C. Chang, H.-P. Wu, Y. Cheng, E. W.-G. Diau and M. Wang, *Phys. Chem. Chem. Phys.*, 2016, **18**, 6885.
7 P. D. Harvey, in *Multiporphyrins, Multiphthalocyanines and Arrays*, eds. K. M. Kadish, K. M. Smith and R. Guilard, (*The Porphyrin Handbook*, vol. 18), Academic Press, Amsterdam, 2003, pp. 63–250.
8 F. Sabuzi, M. Stefanelli, D. Monti, V. Conte and P. Galloni, *Molecules*, 2020, **25**, 133.
9 H.-L. Ma and W.-J. Jin, *Spectrochim. Acta, Part A*, 2008, **71**, 153.
10 G. De Luca, A. Romeo and L. M. Scolaro, *J. Phys. Chem. B*, 2006, **110**, 7309.
11 Y. Zhang, M. X. Li, M. Y. Lü, R. H. Yang, F. Liu and K. A. Li, *J. Phys. Chem. A*, 2005, **109**, 7442.
12 G. De Luca, A. Romeo and L. M. Scolaro, *J. Phys. Chem. B*, 2005, **109**, 7149.
13 J. Mosinger, M. Janošková, K. Lang and P. Kubát, *J. Photochem. Photobiol. A*, 2006, **181**, 283.
14 X. Li, D. Li, M. Han, Z. Chen and G. Zou, *Colloids Surf., A*, 2005, **256**, 151.
15 K. Kano, K. Watanabe and Y. Ishida, *J. Phys. Chem. B*, 2008, **112**, 14402.
16 E. Araya-Hermosilla, M. R. Abbing, J. Catalán-Toledo, F. Oyarzun-Ampuero, A. Pucci, P. Raffa, F. Picchioni and I. Moreno-Villoslada, *Polymer*, 2019, **167**, 215.
17 G. De Luca, A. Romeo, V. Villari, N. Micali, I. Foltran, E. Foresti, I. G. Lesci, N. Roveri, T. Zuccheri and L. M. Scolaro, *J. Am. Chem. Soc.*, 2009, **131**, 6920.
18 I. G. Occhiuto, R. Zagami, M. Trapani, L. Bolzonello, A. Romeo, M. A. Castriciano, E. Collini and L. M. Scolaro, *Chem. Commun.*, 2016, **52**, 11520.

19 Z. Sattar, H. Iranfar, A. Asoodeh, M. R. Saberi, M. Mazhari and J. Chamani, *Spectrochim. Acta, Part A*, 2012, **97**, 1089.
20 N. Sh. Lebedeva, E. S. Yurina, Yu. A. Gubarev, A. N. Kiselev and S. A. Syrbu, *Mendeleev Commun.*, 2020, **30**, 211.
21 N. Sh. Lebedeva, Y. A. Gubarev, E. S. Yurina and S. A. Syrbu, *J. Mol. Liq.*, 2018, **265**, 664.
22 G. Sudlow, D. J. Birkett and D. N. Wade, *Mol. Pharmacol.*, 1975, **11**, 824.
23 O. G. Khelevina, S. V. Rumyantseva, E. V. Antina and N. Sh. Lebedeva, *Russ. J. Gen. Chem.*, 2001, **71**, 1058 (*Zh. Obshch. Khim.*, 2001, **71**, 1124).
24 K. Adachi, Y. Ura and N. Kanetada, *J. Porphyrins Phthalocyanines*, 2018, **22**, 658.
25 N. Sh. Lebedeva, E. A. Mal'kova, A. I. V'yugin, V. E. Maizlish and G. P. Shaposhnikov, *Russ. J. Inorg. Chem.*, 2008, **53**, 261 (*Zh. Neorg. Khim.*, 2008, **53**, 303).
26 L. Zhao, X. Wang, Y. Li, R. Ma, Y. An and L. Shi, *Macromolecules*, 2009, **42**, 6253.
27 S. Liu, C. Hu, Y. Wei, M. Duan, X. Chen and Y. Hu, *Polymers*, 2018, **10**, 494.
28 A. S. R. Koti and N. Periasamy, *Chem. Mater.*, 2003, **15**, 369.
29 J. Valanciunaite, V. Poderys, S. Bagdonas, R. Rotomskis and A. Selskis, *J. Phys.: Conf. Ser.*, 2007, **61**, 1207.
30 M. Rotenberg and R. Margalit, *Biochem. J.*, 1985, **229**, 197.
31 O. Trott and A. J. Olson, *J. Comput. Chem.*, 2010, **31**, 455.
32 M. J. Frisch, G. W. Trucks, H. B. Schlegel, G. E. Scuseria, M. A. Robb, J. R. Cheeseman, G. Scalmani, V. Barone, G. A. Petersson, H. Nakatsuji, X. Li, M. Caricato, A. Marenich, J. Bloino, B. G. Janesko, R. Gomperts, B. Mennucci, H. P. Hratchian, J. V. Ortiz, A. F. Izmaylov, J. L. Sonnenberg, D. Williams-Young, F. Ding, F. Lipparini, F. Egidi, J. Goings, B. Peng, A. Petrone, T. Henderson, D. Ranasinghe, V. G. Zakrzewski, J. Gao, N. Rega, G. Zheng, W. Liang, M. Hada, M. Ehara, K. Toyota, R. Fukuda, J. Hasegawa, M. Ishida, T. Nakajima, Y. Honda, O. Kitao, H. Nakai, T. Vreven, K. Throssell, J. A. Montgomery, Jr., J. E. Peralta, F. Ogliaro, M. Bearpark, J. J. Heyd, E. Brothers, K. N. Kudin, V. N. Staroverov, T. Keith, R. Kobayashi, J. Normand, K. Raghavachari, A. Rendell, J. C. Burant, S. S. Iyengar, J. Tomasi, M. Cossi, J. M. Millam, M. Klene, C. Adamo, R. Cammi, J. W. Ochterski, R. L. Martin, K. Morokuma, O. Farkas, J. B. Foresman and D. J. Fox, *Gaussian 09, Revision A.02*, Gaussian, Inc., Wallingford CT, 2009.

Received: 28th May 2020; Com. 20/6228